IL NUOVO CIMENTO VOL. 13 D, N. 4 Aprile 1991

Mechanical Alloying of the Fe-Zr System. Correlation between Input Energy and End Products.

N. BURGIO, A. IASONNA, M. MAGINI(*), S. MARTELLI and F. PADELLA
Amorphous Materials Project, TIB/ENEA, CRE
Casaccia, Via Anguillarese, Roma, Italia

(ricevuto il 21 Maggio 1990)

Summary. — Kinematic equations describing velocity and acceleration of a ball in a vial of a planetary ball-mill have been derived. The consequent energy transfer from the mill to the system constituted by the powder, the balls and the vials have been evaluated by theoretical-empirical approach. Mixtures of elemental iron and zirconium powders corresponding to the average Fe_2Zr composition have been mechanically alloyed in different milling conditions. The end products strongly depend on the operative milling conditions and a clear correlation between them and the input energy has been found.

PACS 81.20 – Specialized material fabrications and fabrication techniques.

1. – Introduction.

By ball milling pure elements, as well as intermetallic compounds, we realize an energy transfer from the milling tools to the milled powder. The result of such a milling process is nowadays fully documented in current material literature: formation of an amorphous phase from the elements (*e.g.* [1-6]); formation of intermetallics from the elements [7-10] that can subsequently amorphize, in some cases, by further prolonged milling [7, 9]. One refers to the above cases as mechanical alloying. Amorphization of intermetallics has also been described [6, 11, 12]. Finally demixing towards the parent elements and/or towards unknown phases has also been reported when starting from intermetallic compounds [13, 10], or from a previously formed amorphous phase [14, present work].

Ball milling has therefore proved to be an easy tool in order to promote different kinds of solid-state reactions and possibly new materials with peculiar properties. A few papers [15-17] also point out that the products of the milling process strongly

(*) The paper has been partly presented at the SSAR Int. Congress held in Grenoble, 20-23 February 1990 and to the ASM Int. Conference on Structural Applications of Mechanical Alloying, Myrtle Beach, 27-29 March 1990.

depend on the milling conditions. Using different ball mills [15, 17] or different conditions of the same ball mill [16] results in markedly different reactions pathways. These experimental evidences are not at all surprising. Indeed, changing the milling conditions will obviously strongly affect the way by which energy is transferred to the milled powder and hence the nature of the final products.

Up to now, apart from the few scattered results mentioned [15-17], no attempt has been done to carefully correlate the milling operative conditions and the end products. Theoretical-empirical equations for the input energy are given in the following and their correlation with the experimental results of milling are evidenced. The Fe-Zr system is well suited for the present purpose. Previous investigations have shown the possibility of preparing amorphous powder alloys in a wide concentration range [4]. Furthermore amorphous alloys with high Fe content (more than 60% at Fe) exhibit a crystallization temperature of about 680 °C [18]. Thus the effect of a slight warming up of the milling device can be reasonably neglected, the process products only being influenced by the energy transfer during ball impact.

2. – Experimental.

Pure iron (99.999% from Carlo Erba) and zirconium (99.9% Ventron FmbH) powders were mixed to the average Fe_2Zr composition. The mechanical alloying process was carried out in a conventional planetary ball mill (Fritsch Pulverisette *P*5) schematized in fig. 1. Four 250 cc. tempered steel vials were contemporarily used in a given experiment. To avoid oxidation the vials were sealed under pure argon.

The rotation speed of the planetary mill can be varied by a potentiometer and has been evaluated (in rounds per minute) by both stroboscopic and takimetric devices for each potentiometer position. It was found that the rotation speed is independent of the charge of the vial (confirming thus the information from the constructing house; for kinematic parameters of the mill see appendix, point 4).

In order to avoid excessive warming of the vials, two precautions were adopted. One hour of milling consisted of four intervals of 15 min each followed by 30 min of

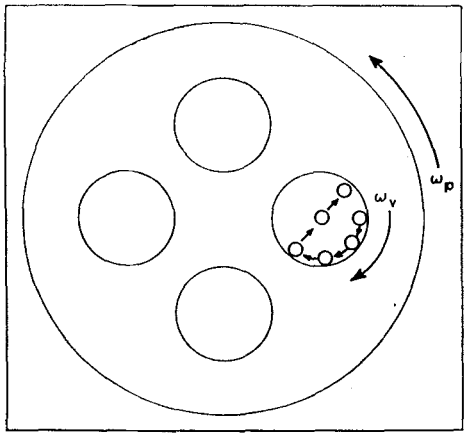

Fig. 1. – Scheme of Fritsch Pulverisette (*P*5) ball mill. W_p and W_v are the nonindependent angular velocities of the ball mill plate and of the vials, respectively.

rest and, both during milling and rest times, compressed air was forced into the mill. By the above procedure we greatly reduced the average increase of temperature of the milling device. We verified, by stopping the ball mill and immediately touching the vials, that the average milling temperature was always kept well below 80 °C even at the maximum rotation speed and charge of the vial.

In order to warrant a statistically representative sampling after each milling period, the following procedure was adopted for all experiments described in the next sections. The vials were open, the balls taken out and the external surface of the vials was struck in order to gently detach as much as possible of the powder attached to the inner walls. The balls were then put back into the vials and run on the mill for few seconds. The new powder removed in this way was added to the previous one and all the powder was run again on the mill without balls for one minute. Few milligrams of the final powder were used to coat a wide adhesive tape surface to perform X-ray measurements.

X-ray diffraction patterns of the samples, prepared as previously described, were recorded by automatic Seifert Pad IV and GSD diffractometers. A sufficient wide angular range ($(10 \div 40)$ in 2θ degrees), in which both iron and zirconium main Bragg's reflection fall, was covered using Mo$K\alpha$ radiation ($\lambda = 0.07107$ nm).

3. – Energy transfer.

We will refer to the planetary ball mill schematized in fig. 1. Figure 6 of the appendix shows the geometry of one vial: indicating by $\overline{W}_p$ and $\overline{W}_v$ the absolute angular velocity of the plate of the mill and of one vial and by $\overline{R}_p$ and $\overline{R}_v$ the vectorial distances from the centre of the mill to the centre of the vial and from the centre of the vial to its periphery, it can be shown that the absolute velocity of one peripheral point P can be expressed by the relation (appendix, point 1)

$$V_p = [(W_p R_p)^2 + (W_v R_v)^2 + 2 W_p W_v R_p R_v \cos\alpha]^{1/2} , \tag{1}$$

α being the angle formed by the $\overline{R}_p$ and $\overline{R}_v$ vectors and $W_v = -1.25\, W_p$ in our planetary ball mill.

Let us now consider the movement of one ball of mass m_b and diameter d_b in the vial. We will assume that the ball moves solidal with the peripheral point P (without rolling or sliding on the inner wall) until it is launched at a given moment against the opposite wall by a given composition of inertial forces. After a short succession of hits with the inner wall, the ball becomes solidal again with the wall itself and it is newly accelerated by the vial for the next launch. Let us emphasize that the previous assumptions are highly realistic starting from the moment at which the ball and the inner wall are covered with a thin powder layer.

According to the above hypotheses, the condition for the ball detachment from the inner wall are given by (appendix, point 2))

$$\cos\alpha_b = -W_v^2 R_v / W_p^2 R_p , \tag{2}$$

so that, combining eqs. (1) and (2) and considering the finite diameter d_b of the ball, the absolute velocity of one ball leaving the wall is given by

$$V_b = [(W_p R_p)^2 + W_v^2 (R_v - d_b/2)^2 (1 - 2W_v/W_p)]^{1/2} . \tag{3}$$

The condition for the ball to become solidal again with the wall is given by (appendix, point 2))

$$\cos \alpha_s \simeq 1 , \tag{4}$$

so that the velocity of the ball, after the hits, V_s, equals that of the inner wall and can be expressed, combining eqs. (1) and (4), by

$$V_s = [(W_p R_p)^2 + W_v^2 (R_v - d_b/2)^2 + 2 W_p W_v R_p (R_v - d_b/2)]^{1/2} . \tag{5}$$

We have to consider now the mechanism of energy transfer. When the ball is launched, it possesses the kinetic energy

$$E_b = (1/2) m_b V_b^2 \tag{6}$$

and during the first collision event a fraction of this kinetic energy is released. The energy release manifests itself as deformation of the materials and instantaneous rise of temperature and concerns i) the ball, ii) the surrounding region of the hited wall point, iii) the powder trapped between the ball and the wall. These objects constitute the «system» on which energy is transferred by the mill.

After a short succession of hits, during which decreasing fractions of kinetic energy are released, the ball's residual energy becomes

$$E_s = (1/2) m_b V_s^2 \tag{7}$$

and the total energy released by the ball during the series of collision events is given by

$$\Delta E_b = E_b - E_s = -m_b [W_v^3 (R_v - d_b/2)/W_p + W_p W_v R_p](R_v - d_b/2) . \tag{8}$$

In a real experiment we are dealing with a finite number of balls, N_b, that hinder each other so that expression (8) must be modified by an empirical factor able to account for the degree of filling of the vial. This factor, φ_b, can be empirically expressed by suitable analytical relations and we have formulated one in the appendix (point 3)). Here we want to explicitate its meaning at the two limiting cases: i) when the vial is completely balls filled, no movement at all is possible and $\varphi_b = 0$; ii) on the opposite $\varphi_b = 1$ for only one or few balls. Considering this factor expression (8) becomes in a real experiment

$$\Delta E_b^* = \varphi_b \Delta E_b , \tag{9}$$

where now ΔE_b^* represents the energy released by one ball in a system containing N_b balls and a given amount of powder.

The total power, P, transferred from the mill to the system during collisions, can be expressed as

$$P = \varphi_b \Delta E_b N_b f_b , \tag{10}$$

where $f_b = K(W_p - W_v)/2\pi$, the frequency with which balls are launched, is proportional to the relative speed of rotation of the mill (appendix, point 3)). Therefore, we have

$$P/K = \varphi_b \Delta E_b N_b (W_p - W_v)/2\pi \tag{11}$$

or, multiplying by the milling time, t, and normalising by the weight of the powder, PW

$$(12) \quad P^* = (Pt/K\,\mathrm{PW}) = \\ = -\varphi_b N_b m_b t(W_p - W_v)[W_v^3(R_v - d_b/2)/W_p + W_p W_v R_p](R_v - d_b/2)/2\pi\,\mathrm{PW}\,.$$

We want to point out that, to derive the previous «hit model» equations, we have done the severe assumption that energy is only released by collisions between balls and walls. Further the energy release given by eq. (8) and subsequent ones concerns, we remember, the balls, the walls and the powder, while the energy transfer we are interested in is the one from the balls to the powder trapped during collisions which is obviously only a fraction of the total energy release considered in the model.

In spite of the indicated restrictions, we will see that the model described is able to rationalize most of the experimental results reported in the following.

We want finally to outline that the parameters that can be freely varied in eq. (12) are the number, N_b, and the mass, m_b, of the balls (*i.e.* for a given material the total ball weight and the diameter), the angular velocity of the mill, W_p, and the milling time t. The total weight of the powder, PW, can also be freely varied, or can be fixed if the weight ratio balls to powder is kept constant. In the next section the total weight of the powder, the rotation speed, the ball diameter and the time have been considered as variable parameters while the weight ratio was kept constant to about ten.

4. – Analysis of the results.

The main goal of this work was to correlate the input energy from the mill and the products obtained. For a clear understanding of the results shown in the following, we anticipate that we have identified several typical situations to occur during the milling process of the Fe-Zr system and we will refer to them as

a) Line broadening. The main effect of the milling process is only a broadening of the X-ray lines of the starting iron and zirconium components.

b) Formation of an amorphous phase. Disappearance of the initial X-ray lines and appearence of a rather symmetric broad halo centred at ~ 18.6, 2θ degrees ($28.6\,\mathrm{nm}^{-1}$) in agreement with the previous measurements on amorphous powder of the same composition [6, 18], has been assumed as formation of a «true» amorphous phase.

c) Formation of an amorphous intermetallic-like phase. The broad halo grows highly asymmetric around 19.2, 2θ degrees ($s = 29.5\,\mathrm{nm}^{-1}$), where the main reflection of the Fe_2Zr cubic intermetallic phase is expected to occur (ASTM 18-666). Clear evidence of the Fe_2Zr intermetallic phase formation has been detected in some cases and indicated accordingly.

d) Demixing process. Reappearence of broadened X-ray lines (of both known and unknown phases) on the already previously formed amorphous halos has been sometimes observed and indicated as the occurrence of a demixing phenomenon.

Intermediate situations have been properly classified whenever possible, otherwise the dominant situation has been assumed.

4·1. *Absolute weight of the powder.* – Keeping constant RPB (ratio of the weights balls/powder), and the rotation velocity of the mill (equal to 9/10 of the potentiometer scale), we varied the degree of filling of the vials, that is the powder weight and the

corresponding weight of the balls (diameter of the balls $d_b = 10$ mm). Typical results are shown in fig. 2*a*)-*e*) for various degrees of filling.

Some main features can be outlined looking at fig. 2. For the maximum degree of occupancy (PW = 90, weight of the balls 900 g) 225 balls have been used and the vial resulted filled up to about 3/4 of its volume. Movements of the balls are highly

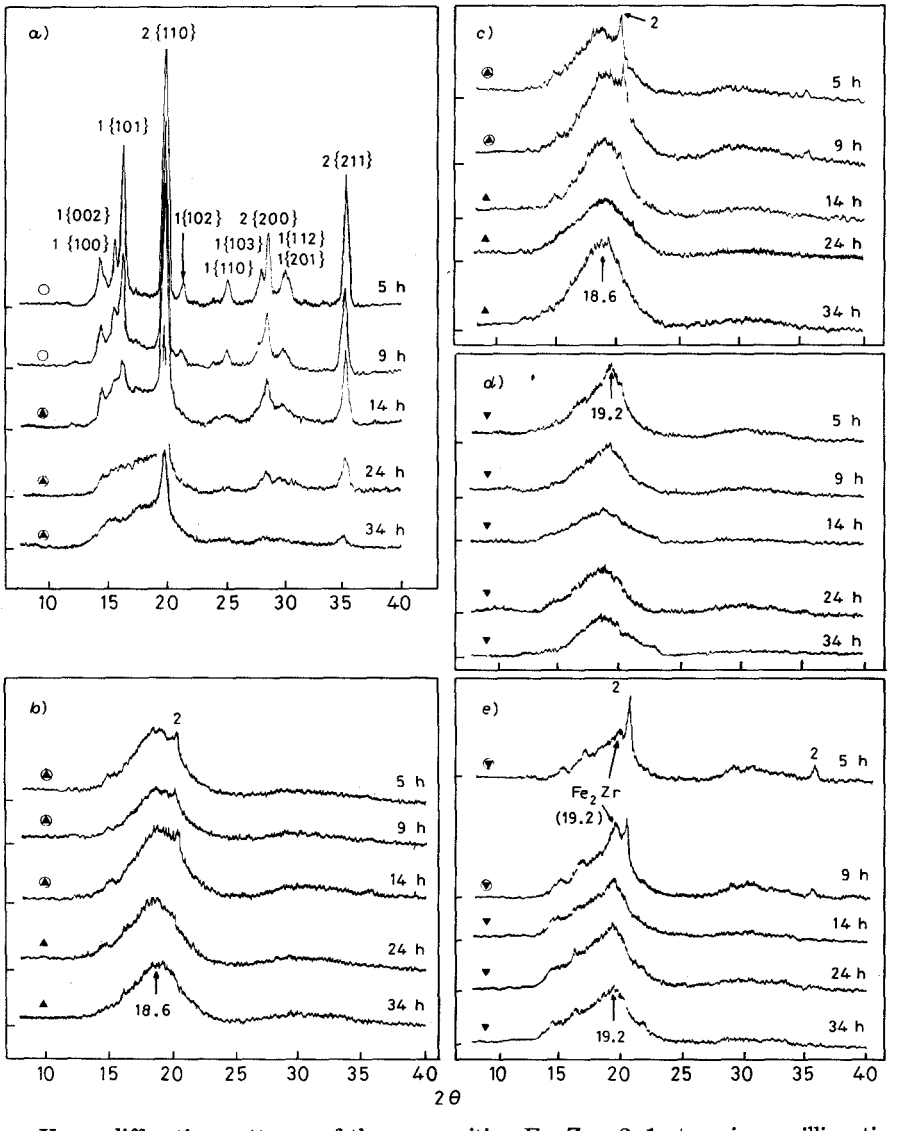

Fig. 2. – X-ray diffraction patterns of the composition Fe : Zr = 2 : 1 at various milling times for different starting weights of the component mixtures PW (powder weigth in grams). (*a*) PW = 90, *b*) PW = 60, *c*) PW = 30, *d*) PW = 15, *e*) PW = 5). In all cases $W = 9$ (ball mill rotation speed expressed in potentiometer arbitrary scale) and $d_b = 10$ (ball diameter in mm) have been used. Each pattern of this figure, and of fig. 3 and 4, has been classified by a symbol indicating (see the text) ○ line broadening, ▲ formation of an amorphous phase, ▼ formation of the intermetallic Fe_2Zr or of an amorphous intermetallic-like phase, □ demixing. Mixed symbols are self-explaining. In each pattern, 1 and 2 indicate the peak position of Zr and Fe, respectively.

hindered in this situation and the energy transfer is expected to be low. In fact, only after 24 h of milling the growth of an amorphous halo is evident (fig. 2*a*)).

Lowering the degree of filling results in a more efficient energy transfer; almost complete amorphization has been reached after 14 hours for PW = 60 and PW = 30 (see fig. 2*b*) and *c*)). In both cases the amorphous halos are centred at ~ 18.6, 2θ degrees, and are quite symmetric. The situation is the one we have classified as formation of a «true amorphous» phase.

Still lowering the occupancy of the vial (PW = 15 and PW = 5), the reaction rate does not change significantely from PW = 60/30, but the growth of the amorphous

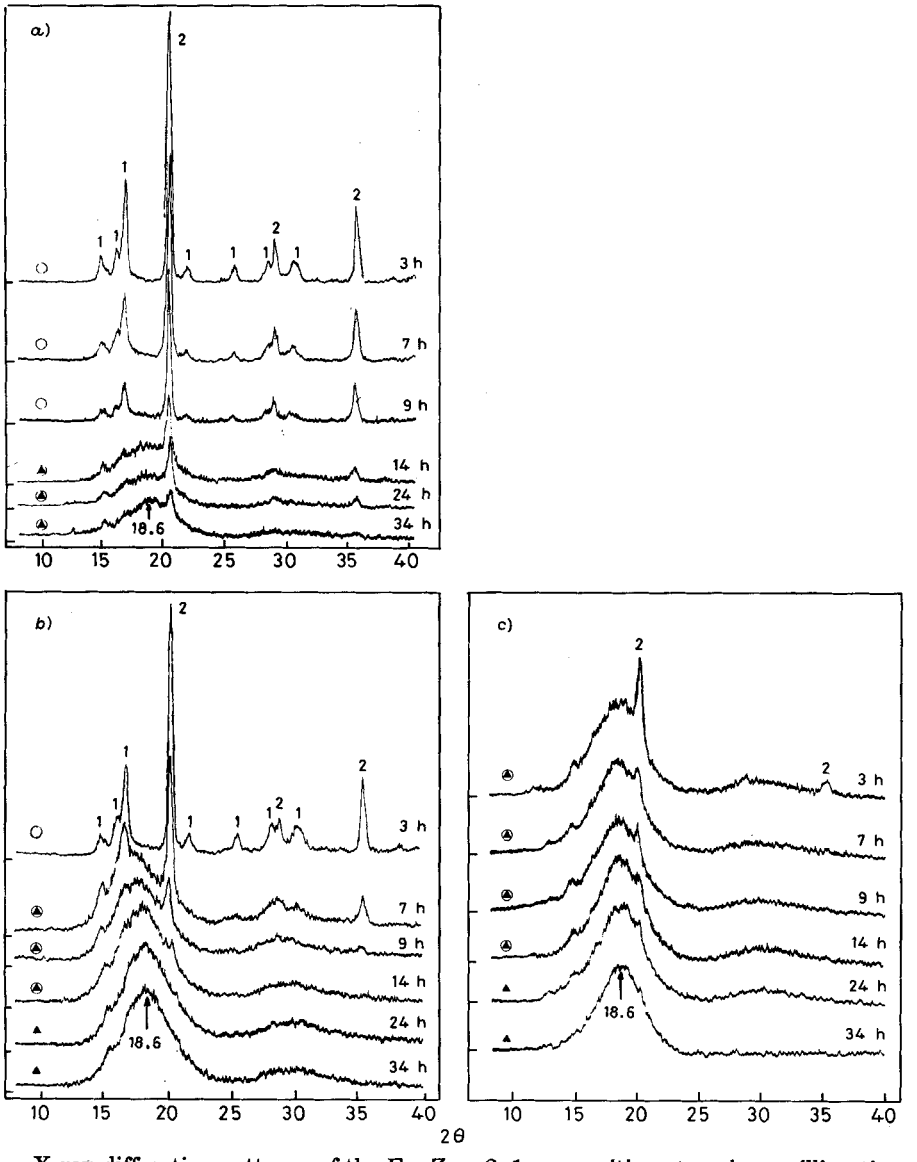

Fig. 3. – X-ray diffraction patterns of the Fe : Zr = 2 : 1 composition at various milling times for different rotation speeds of the ball mill. See fig. 2 for symbols explanation. *a*) $W = 5$, *b*) $W = 7$, *e*) $W = 9$. PW = 40, $d_b = 10$.

halos is now peaked around the {311} main peak of the Fe_2Zr phase (2θ degrees 19.2). This phase is clearly evident for the lowest degree of filling (PW = 5) at 5 and 9 hours. In all the other cases of fig. 2*d*) (PW = 15) and 2*e*) (PW = 5) the broad amorphous halos are asymmetric and the maxima approximately lie on the expected position of the intermetallic phase. This is the situation that we have called formation of an «amorphous intermetallic-like» phase.

PW = 20 and PW = 40 have also been explored: the former is very similar to PW = 15 and the latter is shown within the next figure.

4·2. *Rotation speed.* – By keeping constant RBP = 10 and PW = 40 and using balls of 10 mm, we varied the rotation speed of the mill. The results from three different rotation speeds (given in fig. 3 as $W = 5$, 7 and 9/10 of the potentiometer arbitrary scale) are shown in fig. 3*a*), *b*) and *c*).

The effect of using different velocities with the same degree of filling clearly results in different amorphization rates. For $W = 9$, amorphization is almost completed in 7 hours while 14 hours are needed to reach the same level obtained with $W = 7$. For $W = 5$ after 34 hours complete amorphization is not still reached.

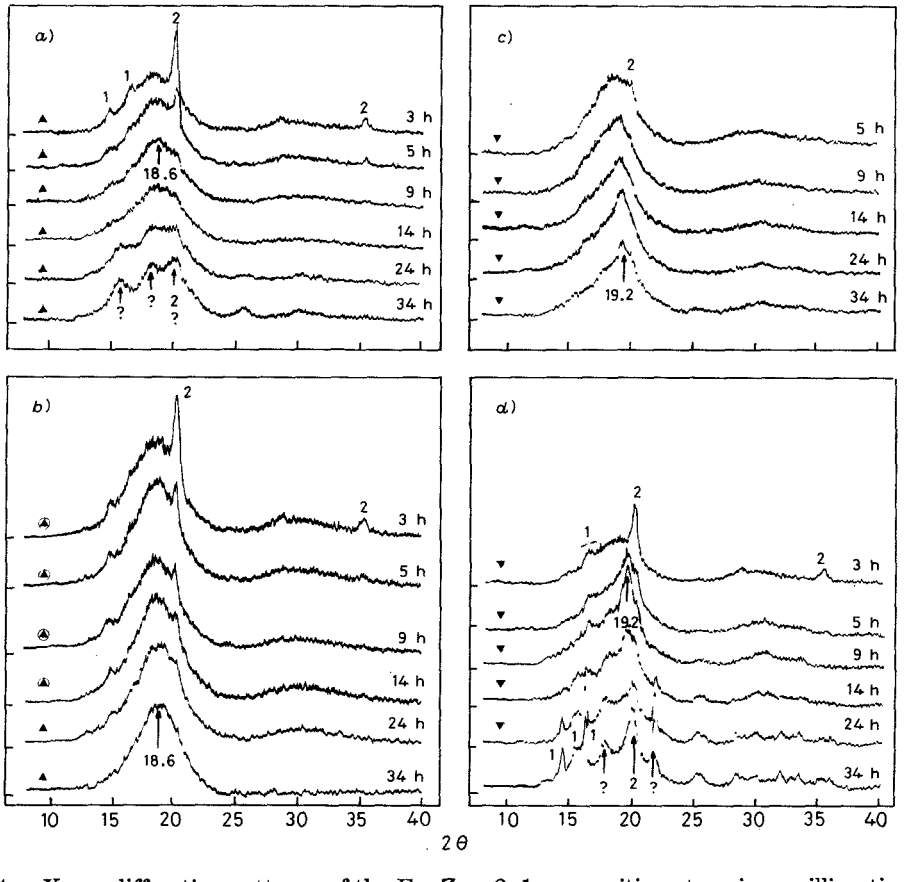

Fig. 4. – X-ray diffraction patterns of the Fe : Zr = 2 : 1 composition at various milling times for different ball diameters. See fig. 2 for symbols' explanation. *a*) $d_b = 6$, *b*) $d_b = 10$, *c*) $d_b = 15$, *d*) $d_b = 20$. PW = 40, $W = 9$.

In all cases growth of the amorphous phase occurs around 18.6 2θ degrees, and the amorphous halos are symmetric (see fig. 3*b*) and *c*)).

4·3. *Balls diameter.* – By keeping constant RPB = 10, PW = 40 and $W = 9$, different ball diameters have been used and the results reported on fig. 4*a*)-*d*). In all the four cases of fig. 4 the amorphization rates are not much different. In fact, the increase in the kinetic energy $1/2\, m_b V_b^2$ with increased m_b (*i.e.* d_b) is counterbalanced by the decreasing of the total number of balls with a final resulting effect of similar amorphization rates in all cases.

A differentiation can be noticed instead on the final products obtained with different ball diameters. For $d_b = 6$ mm and 10 mm an amorphous phase peaked around 18.6 2θ degrees is obtained. On the contrary $d_b = 15$ mm and 20 mm give an amorphous halo centred around 19.2 2θ degrees. Finally a demixing process is detected for the longest milling times of $d_b = 6$ mm and $d_b = 20$ mm.

5. – Discussion.

We have reported in the introduction that different solid-state reactions can be promoted by the milling process: amorphization from pure elements and from intermetallics, formation of intermetallics, demixing phenomena. Dealing with the same system in different milling conditions also results in different reaction pathways. In all cases we realize by ball milling an energy transfer and, obviously, the conditions of such a transfer will favour a given reaction with respect to another. The various kinds of reactions that can take place in the milling process are related to

i) The level of energy obtained during a single collision event. This level can be expressed by eq. (6) and the consequent energy release by eqs. (8) and (9) (it should be enhanced that most of the ΔE_b^* energy release occurs in the first hit).

ii) The total energy transferred to the powder that can be expressed by eq. (12).

The level of energy transferred to the powder during a collision can be correlated to the activation energies of the different reactions that can occur. At an higher activation energy of a given reaction a more energetic milling condition should correspond. For a given milling condition, the integral milling time measures then the total energy needed to complete a given reaction.

For short milling times and low level of energy transfer, only broadening of the X-ray lines is noticed. The phenomenon is due to the reduction of the ordered size domains and to the introduction of defects in the starting metal networks.

At higher level of energy transfer, solid-state reactions can occur towards an amorphous or an intermetallic phase. The preferred pathway depends on the activation energies (and hence on the milling conditions) since thermodynamic considerations only will ever favour the formation of a stable crystalline phase.

As far as we know one example is given in the literature about the influence of different levels of energy transfer, in rigorously controlled conditions, on the final products. Ni_xZr_{1-x} mixtures have been investigated by Eckert *et al.* [16] at different rotation speeds in a Pulverisette (P5) ball mill. They noticed that, in order to form Ni-Zr intermetallic compounds, a higher energy (*i.e.* higher rotation speed) was required than the one needed to form an amorphous phase. We have the same

evidence in the present investigation. Formation of the Fe_2Zr intermetallic phase (or amorphous intermetallic-like phase) has been detected when the highest energetic conditions were used, that is for the highest ΔE_b^* values.

Looking at the experiments of fig. 2, for the lowest level of filling of the vial, the expression for ΔE_b is not damped by any occupancy factor (*i.e.* φ_b near to one) and represents therefore, taking all the other milling conditions constant, the highest level of energy release. Formation of the intermetallic Fe_2Zr is indeed observed in the early milling stages of PW = 5 and PW = 15. At higher degree of filling, ΔE_b is damped by a φ_b factor less than one and Fe_2Zr is no more detected for PW = 30 (fig. 2*c*)), 40 (fig. 3*c*)), 60 (fig. 2*b*)) and 90 g (fig. 2*a*)).

Going to the experiments at different rotation speed W_p (fig. 3), they have been performed at PW = 40 where there is not the condition for an intermetallic to form. Consequently the three experiments tend all, by increasing time, to the amorphous phase formation (halos centred at 18.6 2θ degrees) with a rate depending on the rotation speed.

Finally, the experiments with different ball diameters, where m_b and N_b vary in the opposite directions, show the preminence of the m_b value for the largest ball diameters. For $d_b = 20$ mm evidence of Fe_2Zr is noticed at 9 h; for both $d_b = 15$ mm and $d_b = 20$ mm the amorphous halos are centred at $2\theta \simeq 19.2$ degrees.

Figure 5 summarizes all the experiments performed. The y-axis represents the level of energy ΔE_b^* (eq. (9)) while the x-axis, P^* (eq. (12)), gives the integral energy transferred per unit of weight. The resulting map clearly defines different regions where predominancy of a given product can be extablished. The most interesting point is the finding of a ΔE_b^* value, marked in fig. 5 as $\Delta E_b^{\circledcirc}$, above which true amorphous phase is no more obtainable and only intermetallic Fe_2Zr or amorphous intermetallic-like are detected. Below $\Delta E_b^{\circledcirc}$ the amorphous phase can be obtained in shorter or longer milling times depending on the ΔE_b^* level.

With a few of exceptions, probably related to the intrinsic experimental uncertainty of sampling, all the experiments performed can be fairly well fraimed into the energy map. Conversely the energy map can be used to define the experimental conditions to be employed in order to obtain a given final product.

The fact that the regions defined in fig. 5 are «bent» might depend on the assumptions imposed to derive the hit model equations. Actually, the K factor of eq. (11) is surely constant in given milling conditions, that is for each horizontal line of fig. 5, but probably varies from a given condition to another one. Further, a more accurate modelling can be used for better expressing the empirical factor φ_b. Or, better than that, the occupancy factor should be determined by experimental measurements of the power dissipated in the mill for different charges of the vials. In spite of these limitations, the model based on collisions is able to correlate, in a coherent picture, the experimental milling conditions and the end products.

We want to point out that our model predictions are based on the energy released during collisions. Of course, at any given energy release an instantaneous temperature rise (as well as material deformation) does occur and concerns both the milling tools and the powder trapped. Attempts of evaluating such a temperature rise during collisions have been performed [11, 19] and that approach could profitably be compared with ours. The temperature rise is the effect while the energy release is the cause of such a rise. There is not, of course, contradiction on the different approaches; we want to stress that without need of speaking of temperature rise, we are able to fairly well correlate the input energy with the experimental results.

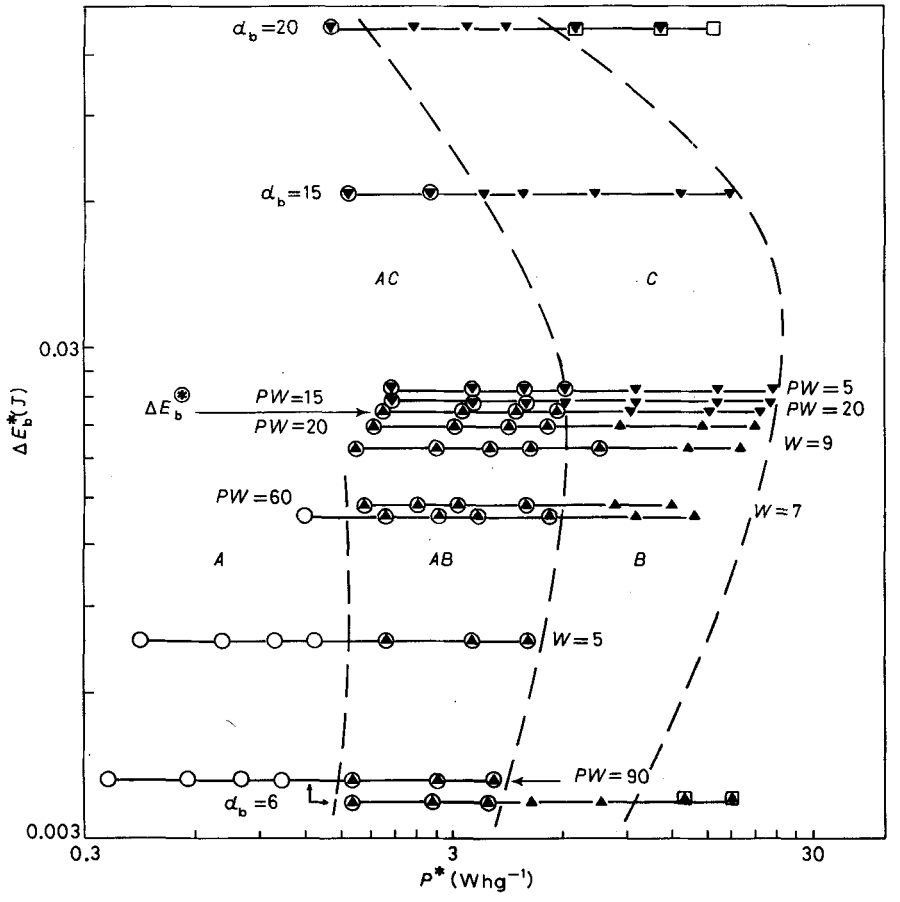

Fig. 5. – Energy map ΔE_b^* (eq. (9), in joules) *vs.* P (*) (eq. (12), watthour per gram) in log-log scale. Each horizontal line represents the level of energy release during collisions of each experimental milling condition and is labelled by one identifying parameter (PW = weight of the powder, W = rotation speed, d_b = ball diameter). On each line seven symbols (see fig. 2) are reported corresponding to the following times: 3, 5, 7, 9, 14, 24 and 34 hours of milling. The level $\Delta E_b^{\circledast}$ represents the level above or below which intermetallics or «true» amorphous phase are formed (see the text). *A*, *B*, *C* regions define conditions where only line broadening (*A*), amorphous phase formation (*B*) and amorphous intermetallic-like phase formation (*C*) are preminent. Regions *AB* and *AC* define self-explained mixed situations. Note that the map includes more patterns than those reported on fig. 2, 3 and 4. The energy levels of PW = 90 and d_b = 6 coincide and have been shifted for clarity. For PW = 60 no sampling could be performed at 3 h.

It must be enhanced that the model has been derived for a planetary ball mill. However, in our opinion, it should be valid for other kinds of ball mills. The movement of the SPEX 8000 ball mill, largely mentioned in the literature, is more complicated (and fixed) and probably equations similar to 1, 3 and 5 are difficult to derive or impossible at all. Still, a correlation between the degree of filling of the vial (N_b and hence φ_b), the materials used (m_b) and the milling time (t) (that is, the

variables explored in the present paper) can be probably extablished and an arbitrary energy scale derived.

A last experimental evidence is worth of mention. In fig. 5 some points refer to the demixing process ($d_b = 6$ mm and $d_b = 20$ mm). This process has been now documented in some cases and is reported to occur for long milling times when starting from intermetallics [15] or for the latest stages of an already performed milling process [10, 14]. In the present case demixing occurs at the two extreme ΔE_b^* levels investigated, that is from an amorphous phase ($d_b = 6$ mm) and from amorphous intermetallic-like phase ($d_b = 20$ mm). The demixing products are different: for $d_b = 20$ mm X-ray lines of the starting components (Fe and Zr) are evident plus unknown peak lines; for $d_b = 6$ mm iron is probably present and the other broad peaks remain nonidentified. Aim of this work is not to deepen this point which surely needs further investigation. We just want to outline here that, since demixing products are different in the two cases mentioned, probably different mechanisms underlie the process.

APPENDIX

Pulverisette ball-mill kinematic and energetic aspects.

Theoretical expressions have been derived for

1) velocity and acceleration of a peripheral point of the inner vial wall,
2) angular position at which one ball detaches from the inner wall and absolute velocity of the ball at the detachment,
3) energy transferred from the mill to the system,
4) kinematic parameters of Pulverisette 5.

1. The pulverisette ball mill is schematized in fig. 1. The geometry of one vial is given in fig. 6 where the following vectorial and scalar variables are defined:

$\overline{R}_p$ = vectorial distance between the centre of the plate 0 and the centre of the vial,

$\overline{R}_v$ = vectorial distance between the centre of the vial H and a peripheral point P of vial wall,

α = angle formed by the $\overline{R}_p$ and $\overline{R}_v$ vectors (angle necessary to anticlockwise superimpose $\overline{R}_p$ on $\overline{R}_v$),

$\overline{W}_p$ = absolute angular velocity of the plate,

$\overline{W}_v$ = absolute angular velocity of the vial.

The relative angular velocity of the vial, with respect to the plate is defined by

$$\overline{W}_r = \overline{W}_v - \overline{W}_p \,, \tag{A.1}$$

the absolute velocity of the point P is defined by

$$\overline{V}_p = \overline{V}_{pr} + \overline{V}_0 \,, \tag{A.2}$$

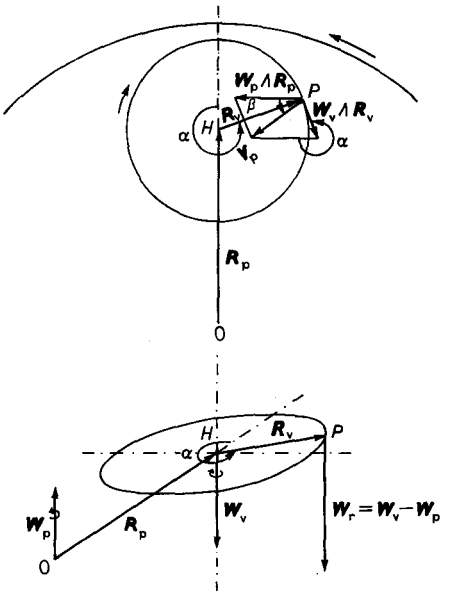

Fig. 6. – Geometry of one vial seen from the top and on perspective. The various vectors and angles are explained in the text.

where

$\overline{V}_{pr}$ = relative velocity of the point P with respect to a reference system solidal with the vial,

$\overline{V}_0$ = absolute velocity of the point of the plate, which is superimposed to the point P of the vial.

By definition it results

$$\overline{V}_{pr} = \overline{W}_r \times \overline{R}_v = (\overline{W}_v - \overline{W}_p) \times \overline{R}_v ,$$

$$\overline{V}_0 = \overline{W}_p \times (\overline{R}_p + \overline{R}_v) ,$$

then

$$\overline{V}_p = \overline{W}_v \times \overline{R}_v + \overline{W}_p \times \overline{R}_p . \tag{A.3}$$

The vector $\overline{V}_p$ is determined by the module V_p and by the angle β formed by $\overline{W}_p \times \overline{R}_p$ and $\overline{V}_p$.

By the vectorial relation (A.3) it is possible to obtain the following analytical expression for the angle β, defined in fig. 6, and V_p module:

$$\cos\beta = \frac{W_p R_p + W_v R_v \cos\alpha}{[(W_p R_p)^2 + (W_v R_v)^2 + 2 W_p W_v R_p R_v \cos\alpha]^{1/2}} , \tag{A.4}$$

$$V_p = [(W_p R_p)^2 + (W_v R_v)^2 + 2 W_p W_v R_p R_v \cos\alpha]^{1/2} , \tag{A.5}$$

where R_v, R_p are the modules of $\overline{R}_v$ and $\overline{R}_p$ and W_p, W_v are scalar values of $\overline{W}_p$, $\overline{W}_v$. By

convention R_v, R_p, W_p are always positive, while W_v is positive or negative, according to the orientation of the $\overline{W}_v$ vector with respect to $\overline{W}_p$ (negative in the case of pulverisette ball mill),

The vectorial acceleration of the point P is given by

$$\overline{a}_p = \mathrm{d}/\mathrm{d}t(\overline{V}_p) = \mathrm{d}/\mathrm{d}t(\overline{V}_{pr} + \overline{V}_0), \tag{A.6}$$

where, by definition, it is possible to write

$$\mathrm{d}/\mathrm{d}t(\overline{V}_{pr}) = \mathrm{d}/\mathrm{d}t(\overline{W}_r \times \overline{R}_v) = \overline{W}_r \times \mathrm{d}/\mathrm{d}t(\overline{R}_v) = (\overline{W}_v - \overline{W}_p) \times \mathrm{d}/\mathrm{d}t(\overline{R}_v),$$

$$\mathrm{d}/\mathrm{d}t(\overline{V}_0) = \mathrm{d}/\mathrm{d}t[\overline{W}_p \times (\overline{R}_p + \overline{R}_v)] = \overline{W}_p \times \mathrm{d}/\mathrm{d}t(\overline{R}_p + \overline{R}_v),$$

since

$$\mathrm{d}/\mathrm{d}t(\overline{R}_v) = \overline{W}_v \times \overline{R}_v\,,$$

$$\mathrm{d}/\mathrm{d}t(\overline{R}_p) = \overline{W}_p \times \overline{R}_p\,,$$

then

$$\overline{a}_p = \overline{W}_v \times (\overline{W}_v \times \overline{R}_v) - \overline{W}_p \times (\overline{W}_v \times \overline{R}_v) + \overline{W}_p \times (\overline{W}_p \times \overline{R}_p) + \overline{W}_p \times (\overline{W}_v \times \overline{R}_v) = -W_p^2 \overline{R}_p - W_v^2 \overline{R}_v\,. \tag{A.6}'$$

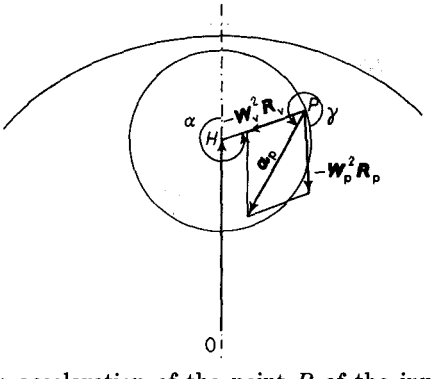

Fig. 7. – Orientation of the acceleration of the point P of the inner vial wall.

The vector orientation of $\overline{a}_p$ is defined by the angle γ formed by $-W_p^2\overline{R}_p$ and $\overline{a}_p$ vectors (see fig. 7). By the vectorial relation (A.6) it is possible to obtain the following system of analytical equations to determine the angle γ and $\overline{a}_p$ module:

$$a_p \sin\gamma = W_v^2 R_v \sin\alpha\,, \tag{A.7}$$

$$a_p = W_p^2 R_p \cos\gamma + W_v^2 R_v \cos(\gamma - \alpha)\,. \tag{A.8}$$

2. The angular position at which one ball detaches from the inner wall is defined by the condition

$$\gamma = \alpha + 90°\,.$$

Defining α_b as the α value at the detachment point, it results

$$\sin\gamma = \cos\alpha_b \,,$$

$$\cos\gamma = -\sin\alpha_b \,,$$

therefore from eq. (A.7) and (A.8)

$$\cos\alpha_b = -W_v^2 R_v / W_p^2 R_p \,. \tag{A.9}$$

The absolute velocity of the balls V_b at the detachment point is determined by replacing, in the analytical expression of V_p (A.5), R_v with $R_v - d_b/2$ (d_b = ball diameter) and $\cos\alpha$ with $\cos\alpha_b$ given by (A.9). Therefore, V_b is defined by the analytical expression

$$V_b = [(W_p R_p)^2 + W_v^2 (R_v - d_b/2)^2 (1 - 2W_v/W_p)]^{1/2} \,, \tag{A.10}$$

where the term $-2W_v/W_p$ is positive in the case of the pulverisette ball-mill.

The inner point of the vial where the first collision between the ball and wall takes place can be evaluated, by geometrical determinations of the trajectory summarized in fig. 8, to be in correspondence of $\alpha_i \cong (360 - 20)$ for point balls. After a few of hits, the ball becomes solidal again with the vial at about $\alpha_s \cong 360°$. Therefore, the absolute velocity V_s, with which the ball starts to move solidal again with the vial, can be assumed, in first approximation, as

$$V_s = [(W_p R_p)^2 + W_v^2 (R_v - d_b/2)^2 + 2W_p W_v R_p (R_v - d_b/2)]^{1/2} \,, \tag{A.11}$$

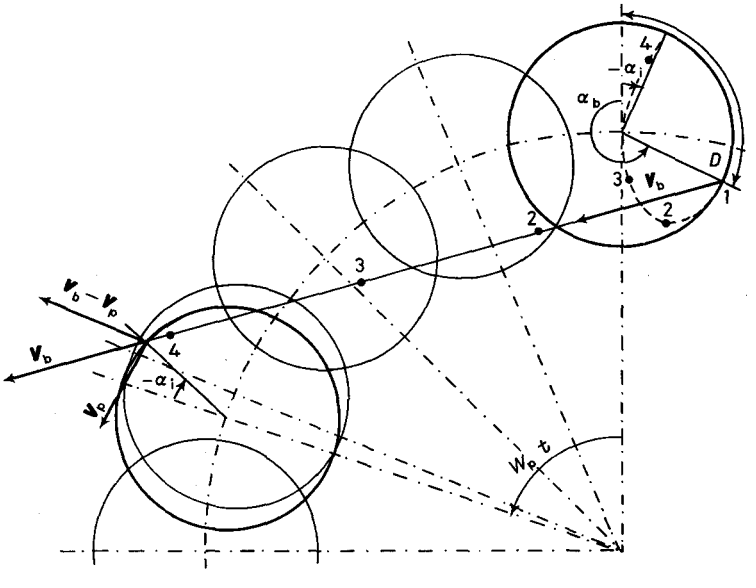

Fig. 8. – Trajectory of one point ball. D denotes the detachment point, α_i denotes the angle of the first collision between ball and wall.

where V_s represents also the absolute velocity of the vials at α_s. The be noticed that in fig. 8 it is indicated that the ball moves solidal with the vial within approximately one third of the inner wall surface.

3. The kinetic energy, E_b, of a single ball launched is given by

$$E_b = (1/2)\, m_b V_b^2 , \tag{A.12}$$

where m_b is the mass of a ball. After the succession of collisions, the kinetic energy becomes

$$E_s = (1/2)\, m_b V_s^2 \tag{A.13}$$

and the energy release

$$\Delta E_b = (1/2)\, m_b (V_b^2 - V_s^2) . \tag{A.14}$$

In the case that N_b balls are used, expression (A.14) must be modified, in order to account for the degree of filling of the vial, by considering a yield coefficient $\varphi_b < 1$. The energy ΔE_b^* dissipated by one ball in a system with N_b ball is given by

$$\Delta E_b^* = \varphi_b \Delta E_b . \tag{A.15}$$

As far as φ_b is concerned, it should be defined by accurate mathematical modelling or by means of experimental measurements. Here we have found convenient to express it as a function of two parameters n_v and n_s:

$$n_v = N_b / N_{b,v} , \tag{A.16}$$

where $N_{b,v}$ is the number of balls that can be contained in a simple cubic arrangement in the vial and is given by

$$N_{b,v} = \pi D_v^2 H_v / 4 d_b^3 , \tag{A.17}$$

D_v and H_v being the diameter and the height of the vial;

$$n_s = N_b / N_{b,s} , \tag{A.18}$$

where now $N_{b,s}$ is the number of balls needed to cover, in a simple cubic arrangement, one third of the inner surface wall and is given by

$$N_{b,s} = \pi (D_v - d_b) H_v / 3 d_b^2 . \tag{A.19}$$

In order to derive a simple analytical expression for φ_b, we will assume that *a)* $\varphi_b = 1$ for $n_v = 0$ (vial completely empty); *b)* $\varphi_b = 0$ for $n_v = 1$ (vial completely filled up) and *c)* φ_b near to 1 (*e.g.* 0.95) for $n_s = 1$ (this assumption means that, until one third of the inner surface wall is not covered, the reciprocal hindering of the ball is negligible). According to these assumptions a simple form for φ_b is given by

$$\varphi_b = (1 - n_v^{\varepsilon}) , \tag{A.20}$$

where ε is a parameter depending on the ball diameter that can be evaluated by

condition *c*):

(A.21) $$0.95 = [1 - (N_{b,s}/N_{b,v})^{\varepsilon}]$$

and it follows for the various ball diameters

(A.22)

diameter (mm)	$N_{b,s}$	ε
6	127	1.3118
10	43	1.6236
15	17	1.9525
20	9	2.1854

Figure 9 shows the φ_b functions.

The total power P transferred from the mill to the system is given by

(A.23) $$P = \Delta E_b^* N_b f_b ,$$

f_b represents the frequency with which the balls are launched against the opposite wall of the vial and can be expressed by

(A.24) $$f_b = K(W_p - W_v)/2\pi ,$$

where K is related to the time necessary to dissipate the energy ΔE_b^* and should not be far from the value of one in the hypothesis of 2-3 collision. Then the final expression for P becomes

(A.25) $$P = -\varphi_b K N_b m_b (W_p - W_v)[W_v^3 (R_v - d_b/2)/W_p + W_p W_v R_p](R_v - d_b/2)/2\pi .$$

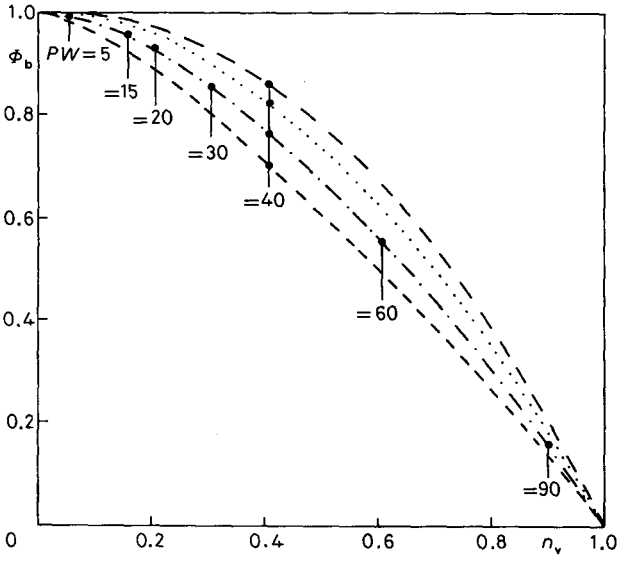

Fig. 9. – φ_b factor *vs.* $n_v = N_b/N_{b,v}$ for four different ball diameters: --- $d_b = 6$ mm, —·— $d_b = 10$ mm, ····· $d_b = 15$ mm, – – – $d_b = 20$ mm.

4. For the Pulverisette *P*5 the geometrical, kinematic and dinamic parameters of the system are as follows:

$R_p = 122.2\,mm$
$R_v = 32.2\,mm$
$W_v/W_p = -1.25$

d_b(mm)	0	6	10	15	20
$\cos\alpha_b$	−0.4117	−0.3734	−0.3178	−0.3158	−0.2839
α_b	−114.3	−111.9	−110.4	−108.4	−106.5
V_b/W_p(m/rad)	0.1435	0.1400	0.1378	0.1352	0.1328
$\cos\beta$	0.9668	0.9703	0.9729	0.9763	0.9797
β	14.8	14.0	13.4	12.5	11.5
$\cos\alpha_i$	0.937	—	—	0.621	—
α_i	−20.4	—	—	−51.6	—
V_{bmax}(*) (m/s)	5.11	4.98	4.91	4.81	4.73

(*) V_{bmax} value at the maximum W_p obtainable in the Pulverisette 5 ($W_p = 35.60$ rad/s = 340 RPM at milling intensity = 10 of the arbitrary potentiometer scale).

REFERENCES

[1] C. C. KOCH, C. B. CAVIN, C. G. MCKAWEY and J. O. SCARBROUGH: *Appl. Phys. Lett.*, **43**, 1017 (1983).
[2] R. B. SCHWARZ, R. R. PETRICH and C. K. SAW: *J. Non-Cryst. Solids*, **76**, 281 (1985).
[3] C. POLITIS and W. L. JOHNSON: *J. Appl. Phys.*, **60**, 1147 (1986).
[4] E. HELLSTERN and L. SCHULTZ: *J. Appl. Phys.*, **63**, 1408 (1988).
[5] A. W. WEEBER and H. BAKKER: *Physica (Utrecht) B*, **153**, 93 (1988).
[6] G. ENNAS, M. MAGINI, F. PADELLA, P. SUSINI, G. BOFFITTO and G. LICHERI: *J. Mat. Science*, **24**, 3053 (1989).
[7] M. S. KIM and C. C. KOCH: *J. Appl. Phys.*, **62**, 3450 (1987).
[8] T. J. TIANEN and R. B. SCHWARZ: *J. Less-Common Met.*, **140**, 99 (1988).
[9] G. ENNAS, M. MAGINI, F. PADELLA, F. POMPA and M. VITTORI: *J. Non-Cryst. Solids*, **110**, 69 (1989).
[10] M. A. MORRIS and D. G. MORRIS: *Solid state powder processing*, in *Proceedings of TMS Conference, Indianapolis, 1-5 October 1989.*
[11] R. B. SCHWARZ and C. C. KOCH: *Appl. Phys. Lett.*, **49**, 146 (1986).
[12] P. Y. LEE, J. JANG and C. C. KOCH: *J. Less-Common Met.*, **140**, 73 (1988).
[13] P. I. LOEFF and H. BAKKER: *Europhys. Lett.*, 8, 35 (1989).
[14] G. COCCO, I. SOLETTA, L. BATTEZZATI, M. BARICCO and S. ENZO: *Philos. Mag.*, **61**, 473 (1990).
[15] A. W. WEBBER, W. J. HAAG, A. J. H. WESTER and H. BAKKER: *J. Less-Common Met.*, **140**, 119 (1988).
[16] J. ECKERT, L. SCHULTZ and E. HELLSTERN: *J. Appl. Phys.*, **64**, 3224 (1988).
[17] E. GAFFET and M. HARMELIN: *Mat. Sci. Eng. A*, **119**, 185 (1989).
[18] E. HELLSTERN and L. SCHULTZ: *Appl. Phys. Lett.*, **49**, 1163 (1986).
[19] R. M. DAVIS, B. MCDERMOTT and C. C. KOCK: *Metall. Trans. A*, **19**, 2867 (1988).